Performance Evaluation of Deep Learning Models for Dental Caries Classification via Panoramic Radiograph Images

Omid Mirzaei[1,2] ID, Bülent Bilgehan[2,3] ID, Mohamad Abduljalil[4] ID, Mhammad Saleh[5] ID, Ammar Kayssoun[5] ID, Ahmet İlhan[2,6] ID

[1] Near East University, Faculty of Engineering, Department of Biomedical Engineering, Mersin, Türkiye.
[2] Near East University, Research Center for Science, Technology and Engineering (BILTEM), Mersin, Türkiye.
[3] Near East University, Faculty of Engineering, Department of Electrical and Electronic Engineering, Mersin, Türkiye.
[4] European University of Lefke, Faculty of Dentistry, Department of Endodontics, Mersin, Türkiye.
[5] Near East University, Faculty of Dentistry, Department of Prosthodontics, Mersin, Türkiye.
[6] Near East University, Faculty of Engineering, Department of Computer Engineering, Mersin, Türkiye.

Correspondence Author: Omid Mirzaei
E-mail: omid.mirzaei@neu.edu.tr
Received: 09.05.2024   **Accepted:** 06.09.2024

ABSTRACT

Objective: The purpose of this study is to evaluate the ability of deep learning models to classify mandibular molar teeth according to the presence and proximity of caries to the dental pulp. This research summarizes the progress of artificial intelligence and potential dental problems in diagnosis, treatment, and disease prediction in medicine. It discusses data limitations, computational power, ethical considerations, and their implications for dentists. This can lay the groundwork for future research in this rapidly expanding field.

Methods: The dataset used in this study consists of 1200 panoramic radiographs, which have been evaluated and classified into three categories: free of dental caries, coded as (H); enamel-dentin caries lesions treated with restorative filling, coded as (R); and deep dental caries that underwent root canal treatment, coded as (E). The images are prepared for the training-testing process using the k-fold cross-evaluation technique and then fed into the pre-trained deep learning models for classification.

Results: The VGG-19 model achieved superior results compared to the other models, with macro-average scores of 0.9111 for precision, 0.9127 for recall, and 0.9115 for f1-score, respectively.

Conclusion: The promising results obtained in this study give confidence in endorsing the use of deep learning models in the dental treatments sector.

Keywords: Artificial intelligence; deep learning; dental caries; panoramic radiology.

1. INTRODUCTION

One of the common chronic oral diseases is dental caries, which mostly affects adults and teenagers worldwide (1). In the United States, the prevalence of dental caries between the age group of children 2-11 years (in primary teeth) is 41%, in children and adolescents 6-19 years of age is 42%, and in adults ≥ 20 years of age (in permanent teeth) is approximately 90 % according to a survey carried out by National Health and Nutrition Examination (2-4). Early detection of dental caries is essential to prevent pulpitis and periapical diseases in advanced stages (5).

Visual tactile inspection and dental radiographs are crucial for detecting dental caries (6). While occlusal surface caries is easily identifiable through direct examination, diagnosing caries in deep fissures, tight interproximal contacts, and secondary lesions is more challenging. As a result, various methods have been developed to improve the detection of dental caries across different anatomical morphologies of teeth (7,8). However, panoramic radiographs are not definitive for diagnosing dental caries due to issues with superimposition and distortion. Still, they were routinely taken during the examination to give a general overview of the dentition and periodontal supporting tissues (9). However, it is considered a good evaluation that may help to reduce the chairside examination time and give the required information about the required diagnostic methods to make the final differential diagnosis (10). Radiographically, dental caries appears as radiolucency in the tooth structure. Mostly, teeth without radiolucency are considered healthy. A small area of radiolucency that does not extend to the pulp chamber indicates the need for a restorative filling. Deep radiolucency, encompassing the pulp chamber, indicates that the tooth requires endodontic treatment (8).

Researchers in the field of artificial intelligence (AI) have come a long way in data processing. AI researchers played a crucial role in data processing (11). The achievements in AI contributed to medical diagnostics (12-14). Medical diagnostics are mostly data problems by nature; therefore, advancements in AI can transform this field (15). The advantage of deep learning is that it extracts details from the input data (16). A sub-category of machine learning known as deep learning takes detailed characteristics out of data (17). This methodology is considered influential in such processing (18). The deep learning offers an accurate solution for various tasks such as Natural Language Processing (NLP), speech recognition and synthesis, signal analysis, and computer vision (19-21). The Convolutional Neural Networks (CNNs), have positive effects on segmentation, object recognition, and classification of various types of images, including medical images (22). Deep learning demands extensive data to achieve an promising result. Transfer learning, a machine learning technique, is implemented to overcome the problem of the limited amount of data. It enables a retraining process with fewer input data that leads to less computational time to achieve more accurate results. According to the chosen model and data, the pre-trained model can lead to acceptable output (23).

The CNN-based applications use dot products of weight matrices and input matrices. A CNN model is divided into two sections: feature learning and classification. Future learning computes the input and future matrices to obtain a feature map. Another critical point is to reduce computational time. Commonly, the pooling operation is adopted to overcome such a problem. The completion of the feature learning and classification process yields the output, as described in the papers (24,25).

This study aimed to evaluate the efficiency and performance of deep learning models to identify the differential diagnosis between three different cases of dental caries depending on the radiographic evaluation of panoramic radiographs to assist the extension of coronal lesions toward the pulp.

2. METHODS

This section presents the collected dataset, the deep learning models considered, and the experimental design.

2.1. Dataset

This study is conducted at the Department of Endodontics, Faculty of Dentistry, Near East University, and received ethical approval from the Scientific Research Ethics Evaluation Board (approval no. YDU/2021/89-1306). The database is collected from the archive between 2018 and 2023 panoramic image files of the dental hospital. The inclusion criteria are based on cases where root canal treatment or restorative filling is performed for one of the lower molars due to a carious lesion. The case selection relied on the diagnosis of the dentist who performed the treatment after establishing professional clinical and radiographic evaluation to improve the diagnosis. Additionally, other healthy mandibular molar teeth in the same patients are included in the study.

The panoramic radiographs previously collected using the X-ray device (Orthophos SL, Sirona, Bensheim, Germany) from the included cases constituted the dataset. These panoramic radiographs are separated from any personal identifiers and anonymized. The collected X-ray image datasets are manually cropped in a standard size to obtain radiographs showing only one molar tooth per image (excluding deciduous teeth) in an optimum position and then calibrated all the images to standardize the contrast between grey/white scales.

The low-resolution radiograph, proximal overlap, retained deciduous, and third molar teeth are excluded from the dataset. 1200 X-ray images including first and second mandibular molars are collected and classified into 400 molars (33.3%) diagnosed as Healthy (non-dental caries), 400 molars (33.3%) diagnosed as enamel-dentin caries, and 400 molars (33.3%) that are diagnosed as root canal treatment. Dental caries were defined as a low-density shadow on dental hard tissue with a rough boundary in the panoramic radiograph. All images were revalidated, and dental caries, including enamel and dentinal carious lesions (excluding deciduous teeth), were distinguished from non-dental caries by calibrated board-certified dentists. The dataset is categorized into three groups: dental caries, which involved the pulp for the teeth underwent root canal treatment (E), caries lesion without pulpal involvement which received restorative filling treatment (R), and healthy molar without caries (H). Figure 1 presents sample images of panoramic radiographs for each group. The dataset is available at https://github.com/ailhan-NEU/Dental-Dataset.
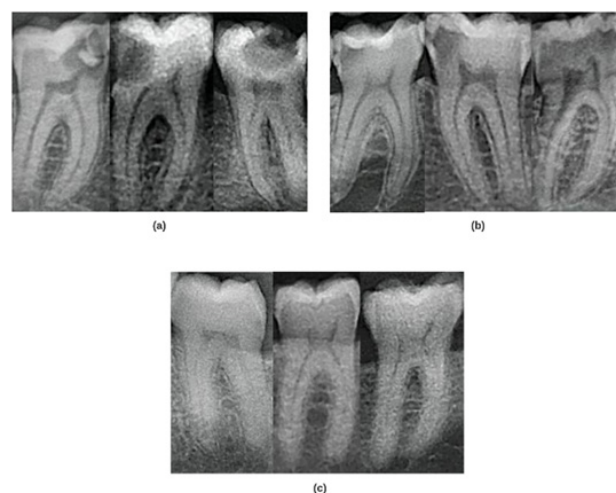
Figure 1. *Examples of panoramic radiography images: (a) Endodontic, (b) Restorative, and (c) Healthy images.*

2.2. Models

In this study, EfficientNet-b0 (26), GoogLeNet (27), Inception-v3 (28), ResNet-50 (29), and VGG-19 (30) deep

learning models are considered for the dental caries classification task.

2.2.1. EfficientNet

The EfficientNet is one of the deep learning models that uses a mixed scaling method. This method allows the width, depth, and resolution dimensions to scale together using a mixed coefficient. There are different models available in EfficientNet, ranging from b0 to b7. The EfficientNet model consists of the Mobile inverted Bottleneck Convolution (MBConv) blocks and squeeze-and-excitation (SE) blocks found in MobileNet-v2. The use of MBConv and SE blocks has been observed to improve accuracy with a small number of parameters.

2.2.2. GoogLeNet

The GoogLeNet was inspired by the pioneering models LeNet and AlexNet but designed as a deeper and more efficient model using a parallel structure and fewer parameters. This design improved the training performance. The success of the GoogLeNet has raised the popularity of deep learning and led to new studies in the field. Therefore, GoogLeNet is a model that has contributed to the significant development of research in deep learning.

2.2.3. Inception

The Inception model is a sophisticated deep learning model renowned for its prowess in image recognition tasks. It employs modules that integrate multiple filter sizes and pooling operations in parallel to capture features at various scales, balancing computational efficiency with high accuracy. Building on this foundation, Inception-v2 incorporates advancements like factorized convolutions and batch normalization. Further refining these improvements, the Inception-v3, introduces additional techniques like label smoothing and auxiliary classifiers, boosting model accuracy.

2.2.4. ResNet

The key innovation of the ResNet is the feature of residual blocks and skip connections. By this feature, higher model accuracy and the problem of gradient loss in weight updates were targeted to be solved. ResNet models uses global average pooling to reduce the size required to process the input. In this way, the depth and the complexity of the model can be increased and the information obtained from each layer will be preserved with skip connections. There are various variants with different depths of the ResNet model, including ResNet-18, ResNet-34, ResNet-50, ResNet-101, and ResNet-152.

2.2.5. VGG

The VGG model shows similarities with the AlexNet, which has an important place among the deep learning models. There are two models available in VGG, 16 and 19. The model consists of sequential convolutional layers, where the filter size increases as the layer depth increases. Research has shown that the performance does not only depend on the increase in filter size but can also be achieved with filters of different sizes. In addition, the smaller filter sizes preferred in the VGG model have been thought to improve the performance by reducing the number of parameters in the training process of the model.

2.3. Experimental Design

The experimental design phase can be summarized in three stages. In the first stage, the images are resized according to the input sizes of considered models to make them suitable for the training and testing process. In the second stage, a k-fold cross-validation (k = 5) technique is applied to determine training and test sets. This technique splits the dataset into k subsets, where in each iteration, one subset is used for testing and the remaining k-1 subsets are used for training. The process is repeated k times, ensuring that each subset serves as the test set exactly once. Lastly, the pre-trained models trained on the ImageNet dataset are fine-tuned using the dental dataset particularly collected for this study. This process enhances their ability to classify dental caries samples by leveraging pre-existing knowledge. The schematic representation of the experimental design is presented in Figure 2.
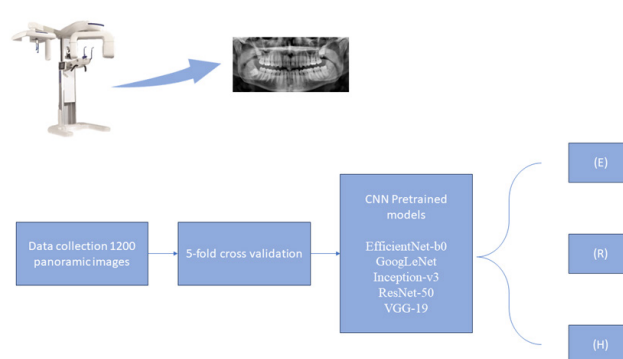
Figure 2. *The block diagram of the experimental design.*

The experiments are carried out via the MATLAB environment. The computer used for the experiments is configured with 32 GB of RAM, an NVIDIA GeForce RTX 2080-Ti GPU, and a 9th generation i9 CPU. Each model is trained using the Adam optimizer with a batch size of 32, a learning rate of 0.0001, and for a maximum of 100 epochs. The performance of the models is evaluated by precision, recall and f1-score metrics. The formulations of these metrics are as follows:

$$\text{Precision} = \frac{TP}{TP + FP} \quad (1)$$

$$\text{Recall} = \frac{TP}{TP + FN} \quad (2)$$

$$\text{F1} - \text{Score} = \frac{2TP}{2TP + FP + FN} \quad (3)$$

Where TP represents true positives, FN represents false negatives, and FP represents false positives.

3. RESULTS

The performance evaluation of the pre-trained models based on five-fold cross-validation is presented in Table 1-5.

Table 1. Performance evaluation of EfficientNet-b0 model based on five-fold cross-validation.

Fold	Class	Precision	Recall	F1-Score
Fold 1	Endodontic	0.8533	0.8767	0.8649
	Healthy	0.8824	0.9146	0.8982
	Restorative	0.8375	0.7882	0.8121
Fold 2	Endodontic	0.8659	0.8452	0.8554
	Healthy	0.8902	0.9241	0.9068
	Restorative	0.7895	0.7792	0.7843
Fold 3	Endodontic	0.8625	0.8415	0.8519
	Healthy	0.7629	0.9250	0.8362
	Restorative	0.7937	0.6410	0.7092
Fold 4	Endodontic	0.8939	0.7973	0.8429
	Healthy	0.8913	0.8817	0.8865
	Restorative	0.7439	0.8356	0.7871
Fold 5	Endodontic	0.8861	0.8046	0.8434
	Healthy	0.7647	0.9848	0.8609
	Restorative	0.8421	0.7356	0.7853
Average	Endodontic	0.8723	0.8331	0.8517
	Healthy	0.8383	0.9261	0.8777
	Restorative	0.8013	0.7559	0.7756

In addition, the confusion matrices of the models are presented in Figure 3.

Figure 3. Confusion matrices of models.

3.1. Comparison of the Model Performances

The ranking of the models is determined according to the macro-averages of the metrics. Evaluation results show that the VGG-19 model achieved superior results and is defined as the 1st ranking model. Table 6 presents the comparative results for the models.

Table 2. Performance evaluation of GoogLeNet model based on five-fold cross-validation.

Fold	Class	Precision	Recall	F1-Score
Fold 1	Endodontic	0.7882	0.9178	0.8481
	Healthy	0.9620	0.9268	0.9441
	Restorative	0.8947	0.8000	0.8447
Fold 2	Endodontic	0.8765	0.8452	0.8606
	Healthy	0.9383	0.9620	0.9500
	Restorative	0.8077	0.8182	0.8129
Fold 3	Endodontic	0.8611	0.7561	0.8052
	Healthy	0.8941	0.9500	0.9212
	Restorative	0.7590	0.8077	0.7826
Fold 4	Endodontic	0.7500	0.8919	0.8148
	Healthy	0.9872	0.8280	0.9006
	Restorative	0.7703	0.7808	0.7755
Fold 5	Endodontic	0.8795	0.8391	0.8588
	Healthy	0.8182	0.9545	0.8811
	Restorative	0.8500	0.7816	0.8144
Average	Endodontic	0.8311	0.8500	0.8375
	Healthy	0.9200	0.9243	0.9194
	Restorative	0.8163	0.7977	0.8060

Table 3. Performance evaluation of Inception-v3 model based on five-fold cross-validation.

Fold	Class	Precision	Recall	F1-Score
Fold 1	Endodontic	0.9333	0.9589	0.9459
	Healthy	0.9302	0.9756	0.9524
	Restorative	0.9620	0.8941	0.9268
Fold 2	Endodontic	0.9059	0.9167	0.9112
	Healthy	0.9367	0.9367	0.9367
	Restorative	0.8816	0.8701	0.8758
Fold 3	Endodontic	0.8333	0.8537	0.8434
	Healthy	0.8295	0.9125	0.8690
	Restorative	0.8382	0.7308	0.7808
Fold 4	Endodontic	0.8481	0.9054	0.8758
	Healthy	0.9362	0.9462	0.9412
	Restorative	0.8806	0.8082	0.8429
Fold 5	Endodontic	0.9512	0.8966	0.9231
	Healthy	0.8205	0.9697	0.8889
	Restorative	0.9125	0.8391	0.8743
Average	Endodontic	0.8944	0.9062	0.8999
	Healthy	0.8906	0.9482	0.9176
	Restorative	0.8950	0.8285	0.8601

Table 4. Performance evaluation of ResNet-50 model based on five-fold cross-validation.

Fold	Class	Precision	Recall	F1-Score
Fold 1	Endodontic	0.9155	0.8904	0.9028
	Healthy	0.9000	0.9878	0.9419
	Restorative	0.9241	0.8588	0.8902
Fold 2	Endodontic	0.9241	0.8690	0.8957
	Healthy	0.9048	0.9620	0.9325
	Restorative	0.8831	0.8831	0.8831
Fold 3	Endodontic	0.9221	0.8659	0.8931
	Healthy	0.9048	0.9500	0.9268
	Restorative	0.8481	0.8590	0.8535
Fold 4	Endodontic	0.9565	0.8919	0.9231
	Healthy	0.9381	0.9785	0.9579
	Restorative	0.8784	0.8904	0.8844
Fold 5	Endodontic	0.9710	0.7701	0.8590
	Healthy	0.7683	0.9545	0.8514
	Restorative	0.8315	0.8506	0.8409
Average	Endodontic	0.9378	0.8575	0.8947
	Healthy	0.8832	0.9666	0.9221
	Restorative	0.8730	0.8684	0.8704

Table 5. Performance evaluation of VGG-19 model based on five-fold cross-validation.

Fold	Class	Precision	Recall	F1-Score
Fold 1	Endodontic	0.9333	0.9589	0.9459
	Healthy	0.9518	0.9634	0.9576
	Restorative	0.9268	0.8941	0.9102
Fold 2	Endodontic	0.9125	0.8690	0.8902
	Healthy	0.9512	0.9873	0.9689
	Restorative	0.8590	0.8701	0.8645
Fold 3	Endodontic	0.8675	0.8780	0.8727
	Healthy	0.9268	0.9500	0.9383
	Restorative	0.8267	0.7949	0.8105
Fold 4	Endodontic	0.8831	0.9189	0.9007
	Healthy	0.9468	0.9570	0.9519
	Restorative	0.8841	0.8356	0.8592
Fold 5	Endodontic	0.9753	0.9080	0.9405
	Healthy	0.9028	0.9848	0.9420
	Restorative	0.9195	0.9195	0.9195
Average	Endodontic	0.9143	0.9066	0.9100
	Healthy	0.9359	0.9685	0.9517
	Restorative	0.8832	0.8629	0.8728

Table 6. Comparison of pre-trained model performances.

Model	Macro Precision	Macro Recall	Macro F1-Score
EfficientNet-b0	0.8373	0.8384	0.8350
GoogLeNet	0.8558	0.8573	0.8543
Inception-v3	0.8933	0.8943	0.8925
ResNet-50	0.8980	0.8975	0.8957
VGG-19	**0.9111**	**0.9127**	**0.9115**

4. DISCUSSIONS

The panoramic radiograph is considered an important tool to identify the abnormalities of the jaws and adjacent tissues (9). In addition, panoramic and periapical radiographs are the main methods for evaluating and diagnosing dental and periapical lesions, except for some specific cases. However, it is considered a very effective method to evaluate the extension of dental caries, which helps to reduce the time of clinical evaluation and determine the required diagnostic method to make a definitive diagnosis (10). Panoramic radiography offers a rapid, simple means of providing a broad overview of both jaws and teeth and is likely to be well accepted by patients and/or study participants. It is, therefore, commonly used in studies. Variables such as number of remaining teeth, restorative therapy, and endodontic treatments are accurately disclosed. Panoramic radiography provides an adequate overview with a low x-ray dose compared to bitewing and periapical radiographs in taking all teeth and surrounding structures in one image (31). Thomas et al. used an electronic caries meter to validate occlusal caries diagnosis from bitewing and panoramic radiographs. There was no difference in overall diagnostic performance between bitewing and panoramic radiographs to diagnose occlusal dentine caries (32). The use of a panoramic radiograph to diagnose caries in a child's mouth during a general diagnosis has a high advantage compared to every effort that needs to be made to take a bitewing radiograph. Furthermore, the patients who have a gagging reflex, patients who cannot open their mouths due to trismus and infection, and disabled or mentally retarded patients (33-34).

Applying computer-aided diagnosis systems in different dental and medical fields has shown promising effectiveness, and the outcomes were improved. Regarding image analysis, such as classification, segmentation, and detection, convolutional neural networks have been developed speedily in recent years and demonstrate excellent performance compared to public research technologies of deep learning (35). However, although deep CNN algorithms have excellent performance and reliability, clinical applications and basic research in the field of dentistry are limited (33). The purpose of this study was to demonstrate the efficacy of a CNN algorithm for the identification and classification of dental caries using panoramic radiographs. Besides the importance of applying AI in many fields, the information regarding using AI to diagnose dental caries from the panoramic radiographs is limited or could not be available in the literature. Thus, comparing and discussing the results of this study with similar previous studies could be restricted and difficult.

In previous research, deep CNN revealed periapical lesions on the data set of 2001 tooth pieces of panoramic radiographs. A custom-made 7-layer deep neural network, parameterized by 4.299.651 weights, was trained and validated via 10 times repeated group shuffling. In that research, the reference test was the majority vote of 6 independent examiners, comparing the sensitivity and the accuracy of the moderately trained deep convolutional neural networks on a limited amount of

data showed a satisfying ability to detect the apical lesions on panoramic radiographs (36).

The same university applied the same data set used in the previously mentioned article in another study to detect periodontal loss on panoramic dental radiographs. A collection of 2001 image segments from panoramic photography has been established. This study revealed that a deep CNN model, which has been trained on a small number of dental radiographs, has similar accuracy in assisting the periodontal loss compared with the control group, which was assisted by certified dentists, despite the advantage of reducing the effort of dentists and reducing the required chairside time during the conventional diagnosis workflow (37).

Similar to our study, the author designed his study by concentrating on the first lower molar. The study's objective was to detect the presence of extra roots on the distal side of the lower first molar, which can directly affect the outcome of endodontic therapy. A total of 760 cone-beam computed tomography (CBCT) images and panoramic radiographs for vital lower molars have been collected from 400 patients for evaluation and training of the model). The CBCT images have been used as a reference to determine the presence of the Extra distal root, and the panoramic images have been used as material for training. The study showed that trained models can make an accurate differential diagnosis for cases with a fourth distal root in the mandibular molar (38).

Lee et al. (39) used 5390 panoramic and 5380 periapical radiographic images from 3 types of dental implant systems to practice convolutional neural networks to recognize the type and brand of the implant. The board-certified periodontist did the reference test for the selected date. The accuracy of the digital system and the board-certified examiner was very close which means that the digital system, after moderate training, was able to recognize the implant and the brand of the implant among the three different brands used in this study.

Lee, in his study (8), similar to our research, trained a model to diagnose cavitated teeth. The evaluation in the study has been done on periapical radiographs for the teeth. In contrast, the dataset has been established by cropping the molar's teeth from panoramic radiographs. The paper (8) demonstrated that the deep CNN model detected dental caries effectively in periapical radiographs. The established model was expected to be one of the most efficient methods for diagnosing dental caries. For this reason, the authors in the present study try to prove the efficiency of the AI technologies to diagnose caries on the panoramic radiograph, considered the most used X-ray imaging during diagnosis in dentistry.

Lee (40) has also published another article for dental diagnosis using deep learning. In the study, the technology of AI has been evaluated in the revelation and diagnosis of three forms of odontogenic cystic lesions, including odontogenic keratocysts, periapical cysts, and dentigerous cysts using cone-beam computed tomography and panoramic radiography images. This study showed that the pre-trained model using cone-beam computed tomography images revealed efficient diagnostic performance. This performance was more significant than that performed by other models using panoramic radiography images significantly.

In another study, a deep learning model was built using DetectNet with DIGITS version 5.0 for detecting vertical root fractures on 300 panoramic radiography data with visible fracture lines. Two radiologists and one endodontist did the reference test. The results showed that the model was suitable for detecting vertical root fractures in panoramic radiographs (41).

Orhan et al. (42) have used deep learning to detect the periapical pathosis on cone-beam computed tomography (CBCT) images. A human observer has done the reference test. The evaluation was done for 153 periapical lesions taken from 109 patients. In this study, the deep CNN was successful in detecting teeth and numbering specific teeth.

In this study, various pre-trained models are used to classify the dental samples as H, R, and E. The VGG-19 model achieved more efficient results compared to the other models.

Panoramic radiograph images are less accurate than periapical and bitewing images for detecting dental caries. However, they offer a rapid and straightforward way to obtain a broad overview of both jaws and teeth, which tends to make them well accepted by patients and study participants. The use of panoramic radiographs, particularly when cropped to include only the lower molar tooth, can impact the performance of the model and present limitations in this study. Therefore, future studies should aim to overcome these limitations by utilizing different types of radiographic images and new-generation deep learning models.

5. CONCLUSION

Deep learning models have been widely applied in caries to identify further treatment requirements. Experimental results obtained from real patient data in this study suggest the usage of deep learning models in identifying E or H treatment similar to the experts with high accuracy and precision. Applications like the one in this study can be useful assistance as an expert opinion for less experienced. With the promising performance of deep learning-based medical image classification, we trust that commercial Computer-Aided Diagnosis systems are not far in the future. It will encourage biomedical scientists to apply deep learning models for solving other challenging research problems in the wide field of medicine.

REFERENCES

[1] Featherstone JD. The science and practice of caries prevention. J Am Dent Assoc. 2000;131(7):887-899. DOI: 10.14219/jada.archive.2000.0307

[2] Amrollahi P, Shah B, Seifi A, Tayebi L. Recent advancements in regenerative dentistry: A review. Mater Sci Eng C Mater Biol Appl. 2016;69:1383-1390. DOI:10.1016/j.msec.2016.08.045.

[3] Beltrán-Aguilar ED, Barker LK, Canto MT, Dye BA, Gooch BF, Griffin SO, Hyman J, Jaramillo F, Kingman A, Nowjack-Raymer R, Selwitz RH, Wu T. Surveillance for dental caries, dental sealants, tooth retention, edentulism, and enamel fluorosis-United States, 1988-1994 and 1999-2002. MMWR Surveill Summ. 2005;54(3):1-43.

[4] Centers for Disease Control and Prevention, National Health and Nutrition Examination Survey (NHANES) 1999–2002, Accessed [20 November 2023]: http://www.cdc.gov/nchs/about/major/nhanes/datalink.htm

[5] Ali AH, Koller G, Foschi F, Andiappan M, Bruce KD, Banerjee A, Mannocci F. Self-limiting versus conventional caries removal: A randomized clinical trial. J Dent Res. 2018;97(11):1207-1213. DOI:10.1177/002.203.4518769255.

[6] Gomez J. Detection and diagnosis of the early caries lesion. BMC Oral Health. 2015; 15 Suppl 1 (Suppl 1): S3.

[7] Moutselos K, Berdouses E, Oulis C, Maglogiannis I. Recognizing occlusal caries in dental intraoral images using deep learning. Annu Int Conf IEEE Eng Med Biol Soc. 2019; 2019:1617-1620. DOI:10.1109/EMBC.2019.885.6553.

[8] Lee JH, Kim DH, Jeong SN, Choi SH. Detection and diagnosis of dental caries using a deep learning-based convolutional neural network algorithm. J Dent. 2018; 77:106-111. DOI: 10.1016/j.jdent.2018.07.015.

[9] Choi JW. Assessment of panoramic radiography as a national oral examination tool: Review of the literature. Imaging Sci Dent. 2011;41(1):1-6. DOI:10.5624/isd.2011.41.1.1.

[10] Dudhia R, Monsour PA, Savage NW, Wilson RJ. Accuracy of angular measurements and assessment of distortion in the mandibular third molar region on panoramic radiographs. Oral Surg Oral Med Oral Pathol Oral Radiol Endod. 2011;111(4):508-516. DOI: 10.1016/j.tripleo.2010.12.005.

[11] Tandon D, Rajawat J. Present and future of artificial intelligence in dentistry. J Oral Biol Craniofac Res. 2020;10(4):391-396. DOI: 10.1016/j.jobcr.2020.07.015.

[12] Haick H, Tang N. Artificial intelligence in medical sensors for clinical decisions. ACS Nano. 2021;15(3):3557-3567. DOI:10.1021/acsnano.1c00085.

[13] Raheja S, Kasturia S, Cheng X, Kumar M. Machine learning-based diffusion model for prediction of coronavirus-19 outbreak. Neural Comput Appl. 2023;35(19):13755-13774. DOI:10.1007/s00521.021.06376-x.

[14] Pang S, Fan M, Wang X, Wang J, Song T, Wang X, Cheng X. VGG16-T: A novel deep convolutional neural network with boosting to identify pathological type of lung cancer in early stage by CT images. Int J Comput Intell Syst. 2020;13(1):771-780. DOI:10.2991/ijcis.d.200608.001.

[15] Sadiq M, Shi D, Guo M, Cheng X. Facial landmark detection via attention-adaptive deep network. IEEE Access, 2019;7: 181.041.181050. DOI:10.1109/ACCESS.2019.295.5156.

[16] Chowdhary CL, Acharjya DP. Segmentation and feature extraction in medical imaging: A systematic review. Procedia Comput Sci. 2020;167:26-36. DOI:10.1016/j.procs.2020.03.179.

[17] Muhammad K, Khan S, Ser JD, Albuquerque VHC. Deep learning for multigrade brain tumor classification in smart healthcare systems: A prospective survey. IEEE Trans Neural Netw Learn Syst. 2021;32(2):507-522. DOI:10.1109/TNNLS.2020.299.5800.

[18] Guo J, He H, He T, Lausen L, Li M, Lin H, Shi X, Wang C, Xie J, Zha S, Zhang Z, Zhang H, Zhang Z, Zhang Z, Zheng S, Zhu Y. GluonCV and GluonNLP: Deep learning in computer vision and natural language processing. J Mach Learn Res. 2020;21(23):1-7.

[19] Arias-Vergara T, Klumpp P, Vasquez-Correa JC, Noeth E, Orozco-Arroyave JR, Schuster M. Multi-channel spectrograms for speech processing applications using deep learning methods. Pattern Anal Applic. 2021;24(2):423-431. DOI:10.1007/s10044.020.00921-5.

[20] Kuschnerov M, Schaedler M, Bluemm C, Calabro S. Advances in deep learning for digital signal processing in coherent optical modems. In 2020 Optical Fiber Communications Conference and Exhibition (OFC) 2020;(pp. 1-3). IEEE.

[21] Işın A, Direkoğlu C, Şah M. Review of MRI-based brain tumor image segmentation using deep learning methods. Procedia Computer Science 2016; 102: 317-324. DOI: 10.1016/j.procs.2016.09.407.

[22] Isin A, Ozdalili S. Cardiac arrhythmia detection using deep learning. Procedia Computer Science 2017;120: 268-275. DOI: 10.1016/j.procs.2017.11.238.

[23] Kc K, Yin Z, Wu M, Wu Z. Evaluation of deep learning-based approaches for COVID-19 classification based on chest X-ray images. Signal Image Video Process. 2021;15(5):959-966. DOI:10.1007/s11760.020.01820-2.

[24] Acharya UR, Oh SL, Hagiwara Y, Tan JH, Adeli H. Deep convolutional neural network for the automated detection and diagnosis of seizure using EEG signals. Comput Biol Med. 2018; 100:270-278. DOI: 10.1016/j.compbiomed.2017.09.017.

[25] Schirrmeister RT, Springenberg JT, Fiederer LDJ, Glasstetter M, Eggensperger K, Tangermann M, Hutter F, Burgard W, Ball T. Deep learning with convolutional neural networks for EEG decoding and visualization. Hum Brain Mapp. 2017;38(11):5391-5420. DOI:10.1002/hbm.23730.

[26] Tan M, Le Q. Efficientnet: Rethinking model scaling for convolutional neural networks. In International conference on machine learning. 2019; (pp. 6105-6114).

[27] Szegedy C, Liu W, Jia Y, Sermanet P, Reed S, Anguelov D, Rabinovich A. Going deeper with convolutions. In Proceedings of the IEEE conference on computer vision and pattern recognition. 2015;(pp. 1-9).

[28] Szegedy C, Vanhoucke V, Ioffe S, Shlens J, Wojna Z. Rethinking the inception architecture for computer vision. In Proceedings of the IEEE conference on computer vision and pattern recognition. 2016;(pp. 2818-2826). DOI:10.48550/arXiv.1512.00567.

[29] He K, Zhang X, Ren S, Sun J. Deep residual learning for image recognition. In Proceedings of the IEEE conference on computer vision and pattern recognition. 2016;(pp. 770-778). DOI:10.1109/CVPR.2016.90.

[30] Simonyan K, Zisserman A. Very deep convolutional networks for large-scale image recognition. 3rd International Conference on Learning Representations. ICLR. 2015:1-14. DOI:10.48550/arXiv.1409.1556.

[31] Sebring D, Kvist T, Buhlin K, Jonasson P; EndoReCo, Lund H. Calibration improves observer reliability in detecting periapical pathology on panoramic radiographs. Acta Odontol Scand. 2021;79(7):554-561. DOI:10.1080/00016.357.2021.1910728.

[32] Mazurowski MA, Buda M, Saha A, Bashir MR. Deep learning in radiology: An overview of the concepts and a survey of the state of the art with focus on MRI. J Magn Reson Imaging 2019;49(4):939-954. DOI:10.1002/jmri.26534.

[33] Ekert T, Krois J, Meinhold L, Elhennawy K, Emara R, Golla T, Schwendicke F. Deep learning for the radiographic detection of apical lesions. J Endod. 2019;45(7):917-922.e5. DOI:10.1016/j.joen.2019.03.016.

[34] Krois J, Ekert T, Meinhold L, Golla T, Kharbot B, Wittemeier A, Dörfer C, Schwendicke F. Deep learning for the radiographic detection of periodontal bone loss. Sci Rep. 2019;9(1):8495. DOI:10.1038/s41598.019.44839-3.

[35] Hiraiwa T, Ariji Y, Fukuda M, Kise Y, Nakata K, Katsumata A, Fujita H, Ariji E. A deep-learning artificial intelligence system for assessment of root morphology of the mandibular first molar on panoramic radiography. Dentomaxillofac Radiol. 2019;48(3):20180218. DOI:10.1259/dmfr.20180218.

[36] Lee JH, Jeong SN. Efficacy of deep convolutional neural network algorithm for the identification and classification of dental implant systems, using panoramic and periapical radiographs: A pilot study. Medicine (Baltimore). 2020;99(26): e20787. DOI:10.1097/MD.000.000.0000020787.

[37] Lee JH, Kim DH, Jeong SN. Diagnosis of cystic lesions using panoramic and cone beam computed tomographic images based on deep learning neural network. Oral Dis. 2020;26(1):152-158. DOI:10.1111/odi.13223.

[38] Fukuda M, Inamoto K, Shibata N, Ariji Y, Yanashita Y, Kutsuna S, Nakata K, Katsumata A, Fujita H, Ariji E. Evaluation of an artificial intelligence system for detecting vertical root fracture on panoramic radiography. Oral Radiol. 2020;36(4):337-343. DOI:10.1007/s11282.019.00409-x.

[39] Orhan K, Bayrakdar IS, Ezhov M, Kravtsov A, Özyürek T. Evaluation of artificial intelligence for detecting periapical pathosis on cone-beam computed tomography scans. Int Endod J. 2020;53(5):680-689. DOI: 10.1111/iej.13265.

[40] Thomas MF, Ricketts DN, Wilson RF. Occlusal caries diagnosis in molar teeth from bitewing and panoramic radiographs. Prim Dent Care 2001;8(2):63-9. DOI: 10.1308/135.576.101322647908.

[41] Clark HC, Curzon ME. A prospective comparison between findings from a clinical examination and results of bitewing and panoramic radiographs for dental caries diagnosis in children. Eur J Paediatr Dent. 2004;5(4):203-209.

[42] Kamburoğlu K, Kolsuz E, Murat S, Yüksel S, Özen T. Proximal caries detection accuracy using intraoral bitewing radiography, extraoral bitewing radiography and panoramic radiography. Dentomaxillofac Radiol. 2012;41(6):450-459. DOI:10.1259/dmfr/30526171.